










A Late Pleistocene coastal ecosystem in French Guiana was hyperdiverse relative to today

Pierre-Olivier Antoine^{a,1} , Linde N. Wieringa^a , Sylvain Adnet^a, Orangel Aguilera^b , Stéphanie C. Bodin^c , Stephen Cairns^d , Carlos A. Conejeros-Vargas^e, Jean-Jacques Cornée^f , Žilvinas Ežerinskis^g , Jan Fietzke^h , Natacha O. Gribenskiⁱ, Sandrine Grouard^d , Austin Hendy^k, Carina Hoorn^l , Renaud Joannes-Boyau^{m,n} , Martin R. Langer^o , Javier Luque^p , Laurent Marivaux^a , Pierre Moissette^q , Kees Nooren^r , Frédéric Quillévéré^r, Justina Šapolaitė^s , Matteo Sciumbata^{l,s}, Pierre G. Vallat^t , Nina H. Witteveen^l , Alexandre Casanova^u , Simon Clavier^v , Philibert Bidgrain^u, Marjorie Gallay^w , Mathieu Rhoné^w, and Arnaud Heuret^{f,u} 

Edited by Nils Stenseth, Universitetet i Oslo, Oslo, Norway; received July 8, 2023; accepted February 15, 2024

Warmer temperatures and higher sea level than today characterized the Last Interglacial interval [Pleistocene, 128 to 116 thousand years ago (ka)]. This period is a remarkable deep-time analog for temperature and sea-level conditions as projected for 2100 AD, yet there has been no evidence of fossil assemblages in the equatorial Atlantic. Here, we report foraminifer, metazoan (mollusks, bony fish, bryozoans, decapods, and sharks among others), and plant communities of coastal tropical marine and mangrove affinities, dating precisely from a ca. 130 to 115 ka time interval near the Equator, at Kourou, in French Guiana. These communities include ca. 230 recent species, some being endangered today and/or first recorded as fossils. The hyperdiverse Kourou mollusk assemblage suggests stronger affinities between Guianese and Caribbean coastal waters by the Last Interglacial than today, questioning the structuring role of the Amazon Plume on tropical Western Atlantic communities at the time. Grassland-dominated pollen, phytoliths, and charcoals from younger deposits in the same sections attest to a marine retreat and dryer conditions during the onset of the last glacial (ca. 110 to 50 ka), with a savanna-dominated landscape and episodes of fire. Charcoals from the last millennia suggest human presence in a mosaic of modern-like continental habitats. Our results provide key information about the ecology and biogeography of pristine Pleistocene tropical coastal ecosystems, especially relevant regarding the—widely anthropogenic—ongoing global warming.

French Guiana | ancient ecosystems | past biodiversity | Last Interglacial | climate change

During the last 2 My, climatic oscillations induced environmental fluctuations that resulted in drastic changes in biotic distribution all over the globe (1–3). For example, global sea level fluctuated up to 120 m between glacial and interglacial maxima, primarily forced by orbital cycles (4, 5). Such fluctuations led to iterative emergences and drownings of low-elevation coastal areas, with deep consequences on marine taxa (3, 6). The Last Interglacial interval (LIG; Marine Isotope Stage [MIS] 5e; 128 to 116 ka) is characterized by up to 4 to 6 m higher sea-level conditions and overall climatic conditions 2 to 4 °C warmer than today (7–10), making this period a deep-time analog for temperature and sea-level conditions as projected for 2100 AD (11). Despite the existence of numerous data available worldwide, very little is known about LIG low-land biotic assemblages near the Equator, their ecology, and biogeography, more especially in the Atlantic region (8, 10–14) (Fig. 1A and Dataset S1). This gap notably prevents from characterizing the tropical Atlantic biotic communities in the penultimate Earth's warm episode (11, 15–17).

The Guianas comprise a vast territory (ca. 2.5 million km²) near the Equator in South America. Today, this region shelters high levels of taxonomic diversity in both terrestrial and aquatic ecosystems (19–21), but we know almost nothing about its past biodiversity (22, 23). Guianese coastal areas are covered by mangrove vegetation and tidally influenced river banks while, more inland, herbaceous swamps and savannas are followed by marsh and evergreen woodlands (24). This dense vegetation further hampers access to potential fossil-yielding outcrops. Guianese coasts are strongly impacted by a huge flux of surface waters of Andean-Amazonian origin (25), termed the Amazon Plume (AP). This north-westward flux strongly structures the composition of recent tropical Western Atlantic biotic communities, without a clue about its role in the past (25–27).

Here, we report a hyperdiverse marine LIG assemblage, separated by a hiatus from younger continental fossil communities, in a section spanning the last ca. 130 ka. This succession was uncovered during the titanic earthworks that were undertaken in 2015 to 2020 for the Ariane 6 ELA4 launching pad (here KOU-AR6) at Europe's Spaceport,

Significance

The Last Interglacial interval (128 to 116 ka) is a remarkable deep-time analog for temperature and sea-level conditions as projected for 2100, that had not been documented in the equatorial Atlantic thus far. Here, we report hyperdiverse fossil communities of coastal marine and mangrove affinities, dating back from this interval and unearthed at the Europe's Spaceport in Kourou, French Guiana. Mollusk assemblages suggest stronger ecological affinities between Guianas and the Caribbean than today. Grassland-dominated pollen, phytoliths, and charcoals from younger deposits in the same sections attest to a marine retreat and dryer conditions during the Last Glacial Period (100 to 50 ka). These records provide key ecological and biogeographic information about Late Pleistocene tropical coastal ecosystems prior to human influence.

The authors declare no competing interest.

This article is a PNAS Direct Submission.

Copyright © 2024 the Author(s). Published by PNAS. This article is distributed under [Creative Commons Attribution-NonCommercial-NoDerivatives License 4.0 \(CC BY-NC-ND\)](https://creativecommons.org/licenses/by-nc-nd/4.0/).

Although PNAS asks authors to adhere to United Nations naming conventions for maps (<https://www.un.org/geospatial/mapsgeo>), our policy is to publish maps as provided by the authors.

¹To whom correspondence may be addressed. Email: pierre-olivier.antoine@umontpellier.fr.

This article contains supporting information online at <https://www.pnas.org/lookup/suppl/doi:10.1073/pnas.2311597121/-/DCSupplemental>.

Published March 25, 2024.

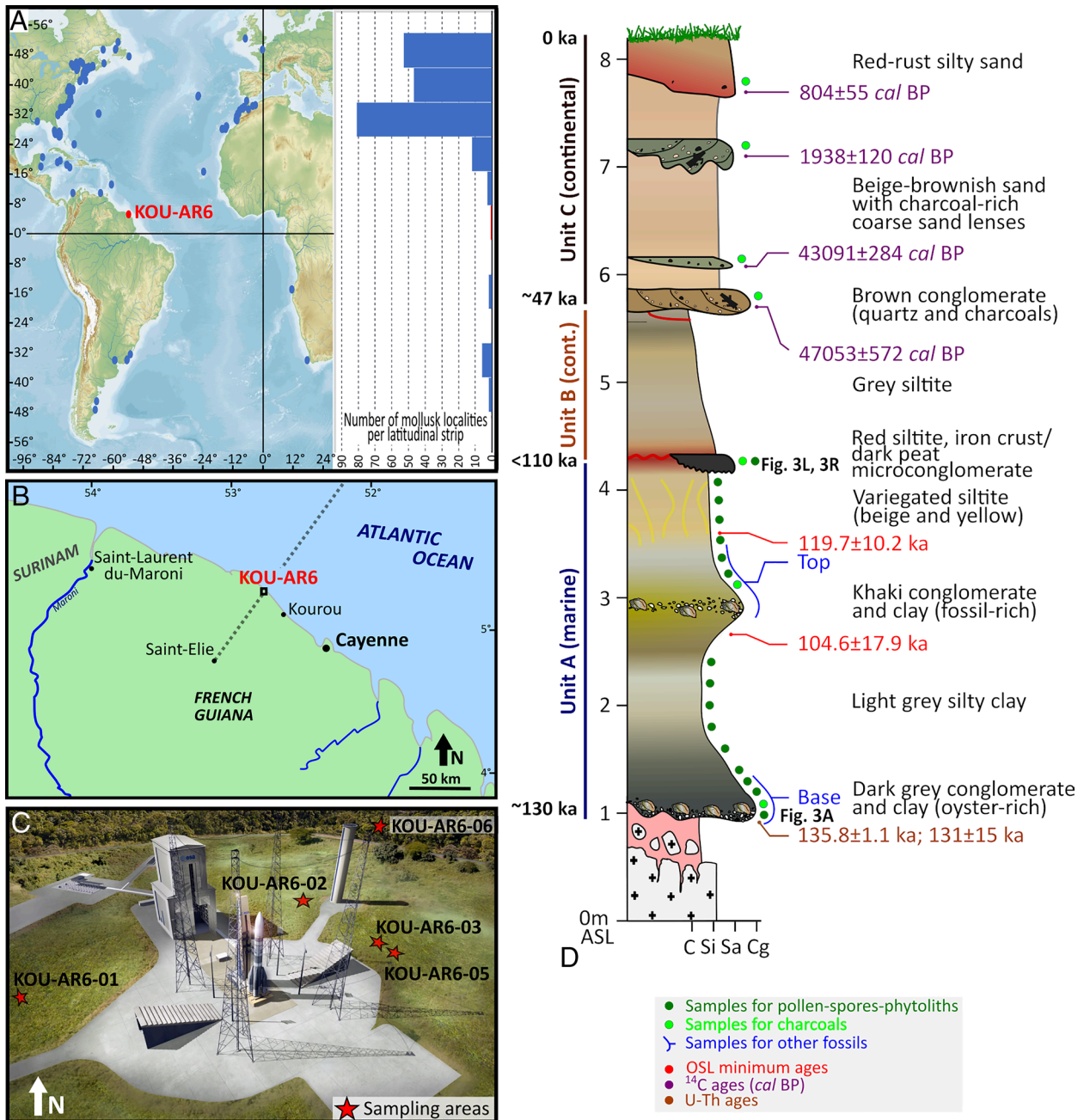


Fig. 1. Location map (A) of the Middle and Late Pleistocene marine mollusk localities, between 60°S and 60°N in the Atlantic Ocean (Dataset S1), as retrieved in the Paleobiology Database (18), and of the Pleistocene–Holocene KOU-AR6 sections and sampling sites (B and C), by the Ariane 6 launcher pad (KOU-AR6-01 to -06). The dashed line denotes the cross-sections as seen in Fig. 4. Composite stratigraphic section (D) at Kourou, French Guiana, with sedimentological descriptions and multi-proxy age constraints. Sampling levels are approximate (for detailed information on each section and sampling efforts, see SI Appendix, Fig. S11). ASL, above sea level; B.P., before present; C, clay; cal, calibrated; Cg, conglomerate; cont., continental; Sa, sand; Si, siltite.

Kourou, French Guiana (FG; Fig. 1 B–D). Our research team includes many specialists from the fields of paleontology and paleobotany to fully reconstruct these ecosystems by using as many different taxonomic groups as possible. As a result, these fossil communities comprise over 270 taxa of foraminifers, metazoans (mollusks, bryozoans, decapods, ray-finned fish, and selachians among others), and plants, further providing a glimpse into the composition of equatorial coastal ecosystems (marine and terrestrial), during both the LIG and the Last Glacial Period (LGP; ca. 115 to 12 ka).

These ancient ecosystems predate human arrival in the Guianas [ca. 10 ka B.P. (28–30)]. They can contribute to testing: i) the regional effects of the global marine retreat related to the LGP; ii)

the behavior of equatorial Atlantic biodiversity during the LIG; iii) the deep history of the AP as a major structuring element of Western Atlantic marine communities; and iv) the relative abundance of now critically endangered marine taxa, in the absence of human footprint.

Results and Interpretation

Pleistocene–Holocene Sections at the Ariane 6 Launch Pad, Kourou, FG. Six trenches and ditches were excavated and investigated for their paleontological content over a 0.5-km² surface in 2019 (KOU-AR6-01 to -05) and 2021 (KOU-AR6-06; Fig. 1C). Common and salient features in these geological sections enabled us to build

an 8-m-thick composite section (*SI Appendix, Figs. S1–S6 and S11*). The base of the section is formed by the top of a Paleoproterozoic granitoid (crystalline basement), which coincides with current sea level (–1/+1 m). The granitoid is overlain by around 0.5 m of pink saprolites (chemically weathered granitoids), followed by a 7-m-thick sedimentary deposit (Fig. 1*D* and *SI Appendix, Fig. S11*). The latter deposit includes three successive units with an erosional base (Units A–C). Based on its fossil content (see below), the lowermost part of this sedimentary ensemble (Unit A, around 4 m thick) is unambiguously of marine origin and referable to the Middle–Late Pleistocene Coswine Formation (Fm.), documented in coastal areas of FG (31, 32).

In all trenches, the fossil-rich ensemble starts by marine deposits (Unit A lying on previously emerged bedrock, transformed into paleosols higher up and topped by an emersion surface, thereby documenting a transgressive/regressive sedimentary cycle). More specifically, Unit A consists of a basal gray oyster-rich conglomerate, transgressive and overlain by gray silty clays (1.5 m). It is covered by a khaki conglomerate in trenches KOU-AR6-03 and -05, with quartz pebbles and oxidized elements, laterally equivalent to khaki or ocher sands in other trenches. Both conglomerates yield calcareous, phosphatic and siliceous, or carbonized marine macrofossils, plus foraminifers and palynomorphs (*SI Appendix*). Above the khaki conglomerate/sand, a regressive sequence starts with 1.5 m of variegated silty paleosols (blueish and ocher or beige and yellow), yielding only siliceous and phosphatized marine fossils (brachiopods and fish; KOU-AR6-06) attesting to their marine origin, with a subsequent weathering due to pedogenesis. These variegated silts become reddish upward and turn into either an iron crust (at KOU-AR6-03, -04 and 05) or a yellow quartz-rich siltite, yielding only continental palynomorphs and phytoliths (at KOU-AR6-06) and topping Unit A. Above it, Unit B is characterized, in all trenches, by around 1.5 m of brownish-orange, gray or yellow silts of continental origin. At KOU-AR6-06, Unit B begins with a 15-cm-thick dark microconglomeratic peat [around 2.5 m above sea level (PN-15a-b pollen and phytolith samples); Fig. 1*D*]. The top of this continental sequence is cut or weathered and replaced by modern soils and human-disturbed surfaces in most of the studied sections. Nevertheless, the KOU-AR6-04 section, culminating 2 to 4 m above all other investigated sections (*SI Appendix, Fig. S11*), provides information on a third unit of fluvial origin, here termed Unit C. This unit consists of 2.5-m-thick beige-brownish coarse sands intercalated with charcoal-rich microconglomeratic lenses and channels.

Age Constraints on the KOU-AR6 Sections. Nineteen samples were dated through independent proxies to estimate the ages of Units A and C (*SI Appendix, Tables S2–S6*). From the base of Unit A (basal conglomerate), aragonitic *Astrangia* corals were dated by U-Th at 131 ± 15 ka by laser ablation and by U-Th at a maximum age of 135.8 ± 1.1 ka by conventional solution multicollector inductively coupled plasma mass spectrometry (MC-ICP-MS; Fig. 1*D*). Higher up in Unit A, quartz-rich silts located 1.7 m above the base of the Coswine Fm. at KOU-AR6-06 were dated through optically stimulated luminescence (OSL) with a minimum age estimate of 104.6 ± 17.9 ka (sample OSL-2). Coswine clays formed a transgressive sequence around the Middle–Late Pleistocene transition (31, 32), further documenting the highest sea level during the LIG [MIS 5e: 128 to 116 ka (9)], and reaching 4 to 6 m above the modern sea level (8, 10). At the top of Unit A, OSL-1, a sample of ocher to beige clayey silts situated 1.1 m above OSL-2, was constrained with a minimum age estimate of 119.7 ± 10.2 ka through OSL dating (corresponding possibly to MIS 5e or to the glacial stadial MIS 5d). For Unit B, there is no radioisotopic dating available, and its age

must be bracketed. Two in situ charcoal samples from successive continental fluvial channels at KOU-AR6-04 provided consistent ^{14}C ages at $47,053 \pm 572$ and $43,091 \pm 284$ calibrated years B.P. [*cal* B.P.], dating the base and the lower part of Unit C, respectively (*SI Appendix, Table S6*). This time span falls within MIS 3, just preceding the LGM within the LGP (9, 33). Drastic climatic changes are recorded during this interval at high and mid-latitudes, but climatic models do consider that no seasonal temperature shift occurred between MIS 3 and the LGM at the Equator (34). The Holocene marine Demerara clays are not recorded in the investigated loci (31, 32). Finally, the two successive riverine channels situated just below the surface at KOU-AR6-04 (top of Unit C) were dated based on charcoals and yielded ^{14}C ages of $1,938 \pm 120$ and 804 ± 55 *cal* B.P. (Fig. 1*D*). At that time, human settlement and land use are well-documented locally (35, 36). Accordingly, the time intervals documented in the KOU-AR6 sections would be ca. 130 to 115 ka (Unit A, marine), ca. 110 to ca. 50 ka (Unit B, continental) and 47 to 1 ka (Unit C, continental).

The Biotic Communities at KOU-AR6 (Pleistocene to Holocene).

All the fossil specimens from the sampled sections are referable to living species, i.e., no extinct taxon is documented thus far at KOU-AR6.

Unit A (ca. 130 to 115 ka), Mangrove to Shallow Marine Environment. Unit A (Fig. 4*A*) documents a very short high sea-level interval spanning the LIG. Based on our chronological constraints, this is most likely MIS 5e, 128 to 116 ka (9). This sequence yielded hyperdiverse assemblages comprising 229 distinct taxa belonging to a wide array of phyla, including foraminifers, mollusks, ray-finned fish, bryozoans, decapods, and sharks among others (Fig. 2), but also plants (charcoals, phytoliths, and pollen; Fig. 3) derived from nearby coastal habitats. In general, mollusks and decapods dominate over other groups, with perfectly preserved delicate shells, pointing to low-energy habitats and preservation in situ.

Foraminifer communities (*SI Appendix, Table S7*) are mainly composed of hyaline-perforate benthic taxa (Fig. 2*A–C*), indicative for shallow intertidal mangrove and subtidal environments (11 species), and one individual of planktonic foraminifer (Fig. 2*D*). The smallest benthic species (*Nonion suburgidum*, *Elphidium magellanicum*, *Cerebrina claricerviculata*, and *Fursenkoina* sp.) usually live in low-oxygenated sediments, while other ones tolerate low-salinity conditions and potentially occur in mangrove habitats and estuaries with variable salinity conditions (*Ammonia*). All other benthic foraminifers are comparatively shallow marine, subtidal taxa, usually occurring in nearshore shallow-water environments with algae or seagrass vegetation. The open ocean influence was probably low. The foraminifers found in all trenches strongly recall the associations observed in a mangrove estuary in northern Brazil, with a significant marine tidal influence (37).

Sponges are only represented by *Entobia* boreholes in oyster shells (Fig. 2*E*). Cnidarians are documented by the octocorallian gorgonian *Pacificorgia*, at KOU-AR6-06 (Fig. 2*G*) and >1,700 specimens of a single scleractinian species, *Astrangia rathbuni*, either growing as solitary corallites or small colonies (Fig. 2*F*). *Astrangia rathbuni* was recognized in all sampled marine levels, with a much higher density at KOU-AR6-06 than in other trenches (*SI Appendix, Table S8*).

The trenches KOU-AR6-01, -03, and -05 yielded 19 species of bryozoans, mostly typical of tropical shallow waters. Most of these taxa also occur in the present-day coastal waters of Brazil (e.g., refs. 38 and 39). Warm-water genera (*Biflustra*, *Steginoporella*, *Antropora*, and *Nellia*) are well represented in both recent and fossil Kourou records. The predominance of encrusting forms

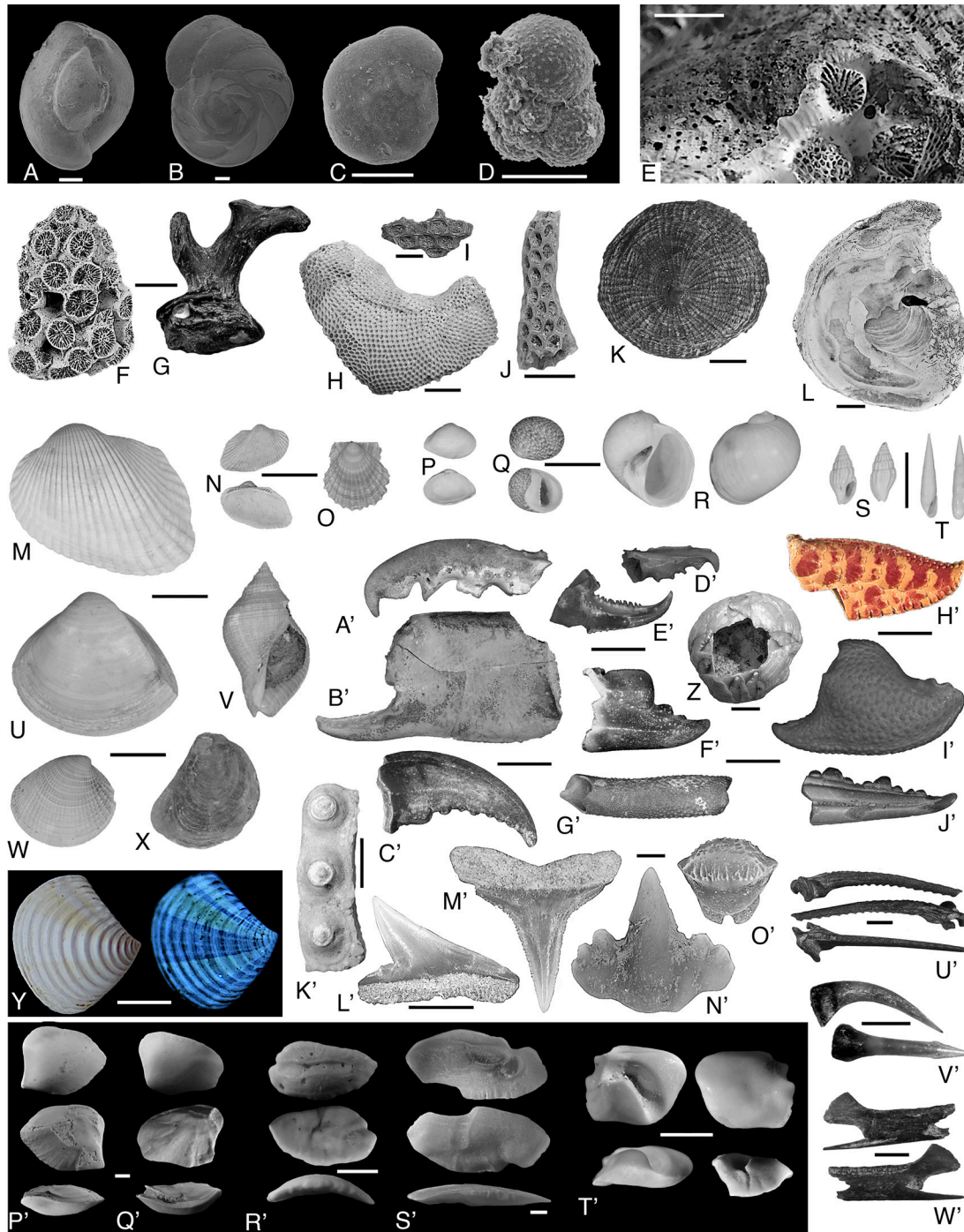


Fig. 2. Marine foraminifer and metazoan communities from Unit A (~130 to 115 ka, Last Interglacial) and associated taxa in KOU-AR6 sections, Kourou, FG. Foraminifers (A–D): (A) *Quinqueloculina seminula* (KOU-AR6-05 Top); (B) *Eponides repandus* (KOU-AR6-03 base); (C) *Ammonia veneta* (KOU-AR6-03 base); and (D) *Globigerina bulloides* (KOU-AR6-05 Top). (E) Detail of an oyster shell, encrusted by bryozoans and a small colony of *Astrangia rathbuni* corals and perforated by *Entobia* sponge boreholes (KOU-AR6-03 base). Cnidarians (F and G): (F) *Astrangia rathbuni*, colony (KOU-AR6-06 base), and (G) *Pacifigorgia* sp., basal portion (KOU-AR6-06 base, 2 mm). Bryozoans (H–J): (H) *Biflustra arborescens* (KOU-AR6-01); (I) *Steginoporella magnilabris* (KOU-AR6-03 Top); and (J) *Conopeum loki* (KOU-AR6-05 Top). (K) Brachiopods, *Discradisca antillarum*, in external view (KOU-AR6-06 Top). Mollusks (L–Y). (L) *Crassostrea* sp., flat (Right) valve in inner view, perforated by pholadid bivalves and *Entobia* (KOU-AR6-02); (M) *Lunarca ovalis* (KOU-AR6-05); (N) *Sheldonella bisulcata* (KOU-AR6-05); (O) *Leptopecten bayayi* (KOU-AR6-05); (P) *Caryocorbula contracta* (KOU-AR6-05); (Q) *Vitta virginea* (KOU-AR6-05); (R) *Stigmaulax cayennensis* (KOU-AR6-05); (S) *Costoanachis avara* (KOU-AR6-03); (T) *Eulima bifasciata* (KOU-AR6-03); (U) *Mulinia cleyana* (KOU-AR6-05); (V) *Stramonita haemastoma* (KOU-AR6-05); (W) *Chione cancellata* (KOU-AR6-05); (X) *Crassostrea rhizophora* (KOU-AR6-03); (Y) *Crassinella lunulata*, under natural light (Left) and 395-nm wavelength UV light (Right). Crustaceans. (Z) Balanomorpha: *Amphibalanus* sp., individual with articulated wall plates (KOU-AR6-01). Axidean (A'–D'), anomuran (E' and F'), and brachyuran decapods (G' and H'). *Neocallichirus* sp., left cheliped dactyl, outer margin (A) and left cheliped propodus, outer margin (B). Callichiridae indet., left cheliped dactyl, inner margin (C) and left cheliped pollex, outer margin (D'). *Pachycheles* sp., left cheliped, outer margin, showing the palm and pollex (E). *Petrolisthes* sp., pollex of right cheliped, outer margin view (F). Eriphioidea (*Eriphia/Menippe*), dactyl of right cheliped, inner margin view (G) and distalmost part of pollex of right cheliped (H). *?Persephona* sp., merus of cheliped indet (I). Portunidae indet., fragment of cheliped pollex (J). Echinoderms. (K') *Arbacia punctulata* (KOU-AR6-06 Base), test fragment. Elasmobranchs (L'–O'). (L') *Isogomphodon oxyrhynchus* (upper tooth); (M') *Rhizopriionodon* sp. (lower lateral tooth); (N') *Ginglymastoma cirratum* (lower tooth); (O') *Hypanus* sp. Bony fish otoliths in rotate views (P' and T'). (P') *Aspistor luniscutis* (KOU-AR6-05 Top); (Q') *Cathorops spixii* (KOU-AR6-05 Top); (R') *Thalassophryne* sp. (KOU-AR6-03 Base); (S') *Macrodon ancylodon* (KOU-AR6-03 Base); (T') *Stellifer rastriifer* (KOU-AR6-05 Top). Bony fish teeth and bones (U'–W'). (U') Erythrinidae indet., tooth (KOU-AR6-03 Base); (V') unidentified freshwater siluriform, pectoral spine (KOU-AR6-03 Base); (W') Nettastomatidae indet., dentary (KOU-AR6-03 Base). [Scale bars, 100 μ m (A–D), 5 mm (E, F, Y, A'–D', G'–I', and M), 2 mm (G, H, F', J', and V), 1 mm (I–K, Z, E', K', L', N'–Q', R'–U', and W), and 10 mm (L–X).]

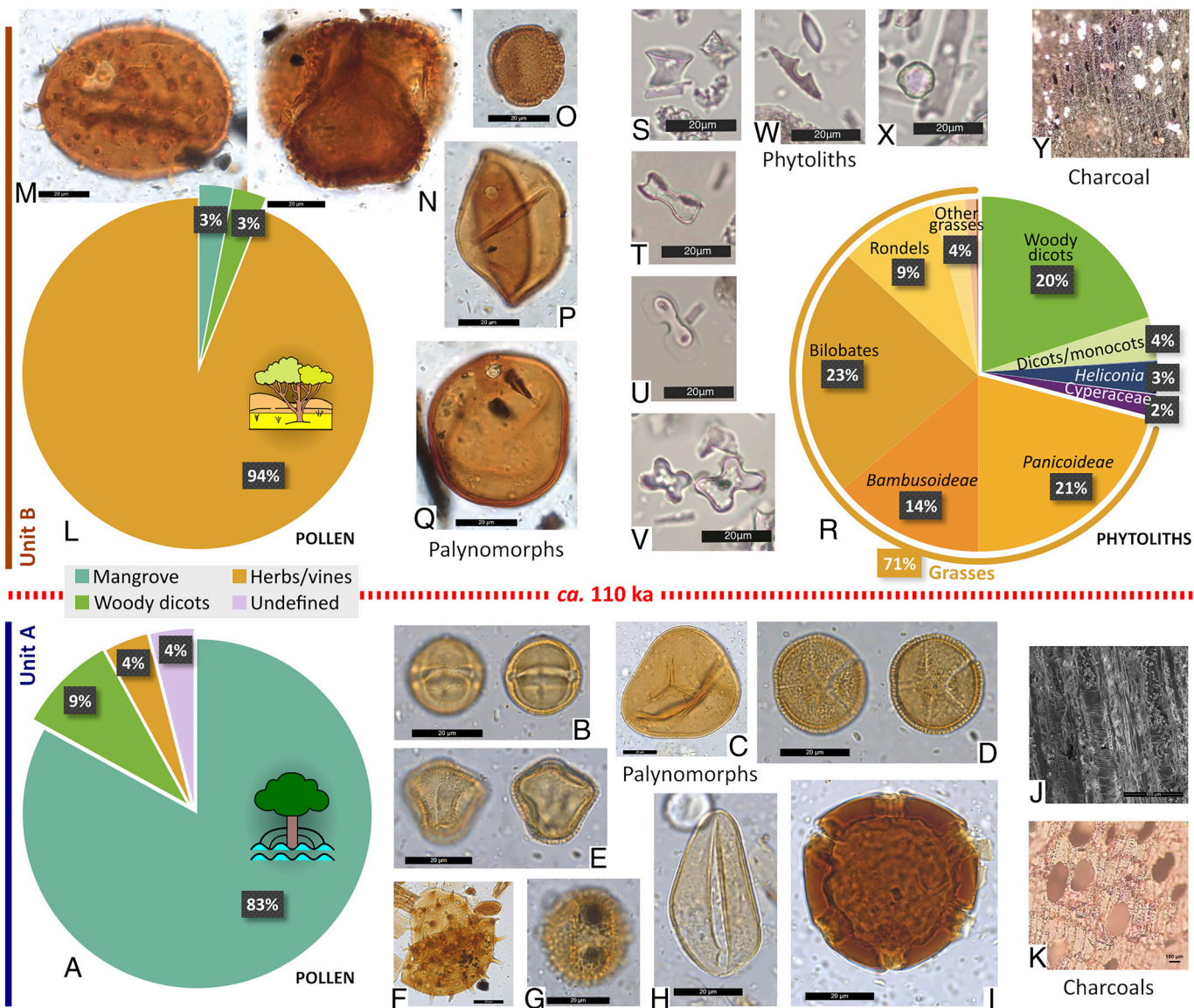


Fig. 3. Pollen and phytolith assemblages and charcoal fragments from Unit A (ca. 130 to 115 ka, Last Interglacial; A–K) and Unit B (LGP (ca. 110 to ca. 50 ka; L–Y) in KOU-AR6 sections, Kourou, FG. (A) Pollen diagram of Unit A (KOU-AR6-PN9), with typical palynomorphs (B–I) and charcoals (J and K); (B) *Rhizophora* sp., red mangrove; (C) *Acrostichum* sp., mangrove fern; (D) *Hedyosmum* sp.; (E) *Schefflera* sp.; (F) *Peltaea* sp.; (G) *Ilex* sp.; (H) *Attalea* type; (I) *Symphonia* sp.; (J) cf. *Rhizophora*; (K) Chrysobalanaceae. (L) Pollen diagram of Unit B (KOU-AR6-PN15), with typical palynomorphs (M–Q); (M) *Mauritia* sp.; (N) *Schultesia* sp.; (O) Rubiaceae indet.; (P) Poaceae indet.; (Q) Poaceae indet.; (R) Phytolith diagram of Unit B with typical phytoliths (KOU-AR6-PN15; S–X) and charcoal (KOU-AR04 Base; Y); (S) Poaceae, rondel; (T) Poaceae, bilobate; (U) Poaceae, *Bambusoideae*; (V) Poaceae, *Panicoideae*; (W) Zingiberales, *Heliconia*; (X) Woody dicot; (Y) cf. *Myrtaceae* (charcoal). [Scale bars, 20 μm (B–E, G, H, M–Q, and S–X), 50 μm (F), or 100 μm (J, K, and Y).]

suggests a shallow depositional environment affected by freshwater influxes associated with increased turbidity, as in mangrove and oyster-rich settings (40).

Around 200 calcareous tubes of unidentified polychaete worms are documented in the marine sequence of all trenches. Siliceous shells of a single brachiopod taxon (*Discradisca antillarum*) are recorded at Kourou, with hundreds of specimens over the entire marine unit and in all sampled trenches.

Mollusks vastly dominate other phyla in both taxonomic diversity and specimen numbers (Fig. 2 L–Y). They include two species of scaphopods (rare), 35 species of bivalves, and 50 species of gastropods. Bivalves and snails are recorded by thousands of individuals in all marine levels that were sampled, with shallow water *Costoanachis avara* (Fig. 2S), *Sheldonella bisulcata* (Fig. 2N), and *Chione cancellata* (Fig. 2W) most abundant. In terms of richness and evenness, KOU-AR6-03 is most diverse with 59 species (SI Appendix, Table S10). The state of preservation is exquisite for

several species which retain colored patterns visible to the naked eye [e.g., *Vitta* (Fig. 2Q), *Pilsbryspiria*] or revealed under UV light [e.g., *Crassinella*, *Olivella*; Fig. 2Y]. Most molluscan taxa have affinities to intertidal and shallow subtidal sands, muds, or rocks and several species are characteristic of mangrove habitats (e.g., *Vitta virginea*, *Isognomon radiatus*).

The crustacean arthropods are particularly dominant at Kourou, with thousands of specimens retrieved from the sediments. All these specimens belong to either barnacles (balanomorph cirripeds), crabs or shrimps (decapods). The barnacles are notably represented by a large amount of disconnected wall plates of *Amphibalanus*, and a single complete specimen (Fig. 2Z). The decapods are represented mostly by hundreds of isolated claw fragments, mainly of mobile and fixed fingers (SI Appendix, Table S11). The decapods comprise eight morphotypes, including two species of mud shrimps (Fig. 2 A'–D'), three species of false crabs, or anomurans (Fig. 2 E' and F'), and three species of true crabs, or brachyurans (Fig. 2 G'–J').

Anomurans include filter feeders found in reefs, under rocks, shell beds, or mangroves. Small claw fragments further document a possible paguroid. The overall decapod association indicates proximity to mangroves, with soft sediments hosting *Neocallichirus* mud shrimps (feeding on seagrass and algae) and purse crabs *Persephona*. This association points to intertidal–subtidal tropical to temperate waters (0 to 50 m), with Western Atlantic, Caribbean, and tropical Eastern Pacific affinities (*Persephona*).

Echinoderms were retrieved in high numbers in all marine samples, nevertheless pointing to a low taxonomic diversity (three species). The echinoderm community is overdominated by the Atlantic purple sea urchin *Arbacia punctulata* (Fig. 2*K*) in all sampled levels and trenches (*SI Appendix, Table S12*). In stark contrast, we retrieved only a few dozens of test fragments of two unidentified heart urchins and two plates of an astropectinid sea star.

No marine mammals or seabirds were preserved, but elasmobranch (sharks and rays; Fig. 2 *L–O*) were identified in all trenches: four species of rays (whipray, eagle ray, saw fish, and cownose ray) and seven species of sharks, including smalltail, daggernose, sharpnose, and lemon sharks, as well as small scoophead hammer sharks and a nurse shark. Daggernose sharks and whiprays dominate the elasmobranch fauna in terms of specimens and occurrences (*SI Appendix, Table S13*). Bony fish are dominantly documented by otoliths (Fig. 2 *P–T*), but also by bones and teeth

(Fig. 2 *U–W*), belonging to 35 species (*SI Appendix, Table S14*). Sciaenid perciforms (16 species, with five distinct *Stellifer*) and ariid siluriforms (eight species) widely outnumber other taxonomic groups in the sample. KOU-AR6-03 is by far the richest locality, with 32 species; *SI Appendix, Table S14*. Thirteen species are recognized in two or three localities, pointing to a certain heterogeneity between the samples (Table 1).

Plant composition and diversity in the marine unit is revealed by fossil charcoals, pollen, spores, and phytoliths (Fig. 3 and *SI Appendix, Tables S15–S17*). As for charcoals, red mangrove (cf. *Rhizophora* sp.), boarwood (cf. *Symphonia globulifera*) and two representatives of Chrysobalanaceae and Myrtaceae were recognized. At KOU-AR6-06, the base of the same unit yielded phytoliths referable to unidentified woody eudicot and Asteraceae, in PN9A and PN9C pollen samples, respectively. The corresponding palynological assemblage (Fig. 3 *A–D*), with a low pollen concentration (around 700 grains cm⁻³), is dominated by *Rhizophora* pollen (80%), followed by spores of the mangrove fern *Acrostichum* (3.5%). No *Avicennia* pollen grains were found. Pollen of tree species accounts for 9% of the pollen sum and reflects the influx of hinterland and lowland (swamp) forest trees (41). Herb and vine pollen is relatively rare (5%) and dominated by Poaceae and Asteraceae. Asteraceae pollen grains were only found in the PN9C sample, also containing one Asteraceae phytolith. The top of this

Table 1. Taxonomic diversity of marine and continental communities from the KOU-AR6 Pleistocene-Holocene sections, Kourou, FG

Higher taxa	Marine	Continental		Total (distinct taxa)
	Unit A ca. 130 to 115 ka	Unit B ca. 110 ka to ca. 50 ka	Unit C 47 to 1 ka	
Foraminifera (foraminiferans)	12	-	-	12
Porifera (sponges)	1	-	-	1
Cnidaria (corals and gorgons)	2	-	-	2
Bryozoa (bryozoans)	19	-	-	19
Annelida (serpulid worms)	1	-	-	1
Mollusca (mollusks)	87	-	-	87
Scaphopoda (scaphopods)	2	-	-	-
Bivalvia (bivalves)	35	-	-	-
Gasteropoda (gastropods)	50	-	-	-
Brachiopoda (brachiopods)	1	-	-	1
Arthropoda (arthropods)	13	-	-	13
Cirripedia (cirripeds)	2	-	-	-
Decapoda (decapods)	11	-	-	-
Echinodermata (echinoderms)	3	-	-	3
Echinoidea (urchins)	2	-	-	-
Asteroidea (sea stars)	1	-	-	-
Vertebrata (vertebrates)	46	-	-	46
Elasmobranchii (rays and sharks)	11	-	-	-
Actinopterygii (ray-finned fishes)	35	-	-	-
Plantae (plants)	41	35	22	92
Charcoal	10	8	22	-
Phytoliths	2	18	-	-
Pollen	30	11	-	-
Total per unit	226	35	22	277

Some plant taxa have been recognized from charcoal and/or pollen in the same unit or in distinct units, hence distinct figures in the last line (distinct taxa per unit) and the last column (distinct taxa identified at KOU-AR6, regardless of the yielding unit).

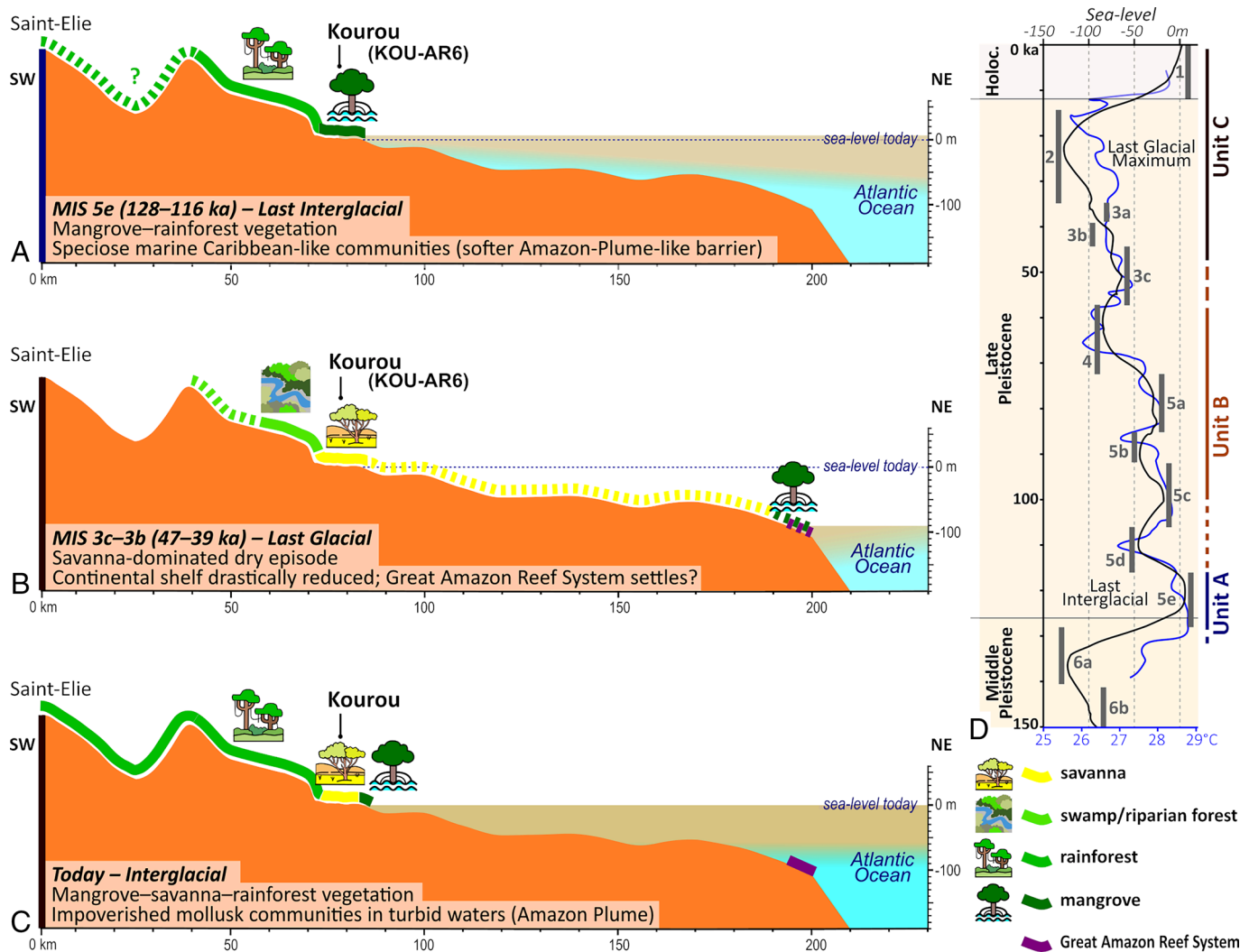


Fig. 4. Hypothesized evolution of Late Pleistocene–Holocene landscapes in FG, using fossil proxies, sedimentary facies, and radioisotopic age constraints available at KOU-AR6 sections, Kourou. (A) During MIS 5e (ca. 130 to 115 ka; Unit A, marine and mangrove settings). (B) During MIS 3c–3b (47 to 39 ka; Unit C, base; continental settings). (C) Today (Unit C, Top, coastal-continental settings). Although documenting fires at its base, Unit B was not sufficiently time-constrained to be satisfactorily depicted here. The presence of a mangrove landscape bordering the Great Amazon Reef System (GARS) at 47 to 39 ka is hypothetical. Main environmental and ecological features related to the sea-level changes, observed locally/regionally over the last climatic cycle, are summarized in the boxes in A–C. (D) Sea-level curve and marine isotopic stages, modified from refs. 4 and 9; sea-surface temperatures modified from ref. 45. The location of the GARS is hypothesized based on ref. 6. For further details regarding age constraints, sampling sections, fossil content, biogeographic/ecological affinities, and corresponding levels, see [Datasets S1–S3](#).

unit has been comprehensively sampled at KOU-AR6-06 for palynomorphs and phytoliths (samples PN10 to 14; [SI Appendix, Table S16](#)). PN10 to 13 only provided a few phytoliths, and PN10 to 14 was also devoid of palynological content. Grass phytoliths first occur at PN12 (dated at 104.6 ± 17.9 ka, OSL-2), with a panicoid cross and a bilobate [C3 and C4 grasses (42, 43)], plus a fused and two rugose spheroids (woody eudicots). PN14 yielded phytolith assemblages dominated by grass phytoliths (70%), as in PN15A–B (base of Unit B, see below).

Unit B (ca. 110–50 ka), Coastal Savanna and Dry forest. Only plant remains were retrieved in this unit.

Tree charcoals were identified at KOU-AR6-04 Base (Fig. 3Y and [SI Appendix, Table S15](#)). The assemblage comprises notably *Hadroanthus* cf. *serratifolius* (ipê) and a close relative, cf. *Drypetes* sp., *Pterocarpus*-like Leguminosae, red mangrove, as well as unidentified Melastomataceae, Myrtaceae-like dicots. Today, these taxa represent trees and shrubs from the primary, riverine or dry forest, savanna, or mangrove and suggest distinct vegetation succession stages at ca. 47 ka *cal* B.P.

The phytolith assemblages counted in the basal dark peat at KOU-AR6-06 (Fig. 3R–X) are dominated by grasses (65%) in both PN15A and PN15B with 65% grass, 31 and 17% woody eudicots, respectively, and almost no palm phytoliths (<1%). Most grass phytoliths encountered are from Panicoideae and Bambusoideae ([SI Appendix, Table S16](#) and Fig. S12). Bilobates and rondels are also common, produced by a wide array of monocot grasses (42, 43). Phytoliths from Pooideae (wavy trapezoids) and Chloridoideae (squat saddles) are rare (<1%). Strikingly, a high percentage of phytoliths were burnt (28%), especially specimens of Cyperaceae, *Heliconia* and Zingiberales. This assemblage suggests that a savanna vegetation had started growing locally way before 50 ka and spread around and settled sustainably. Previous phytolith studies showed that the natural vegetation of seasonally flooded/coastal Holocene savannas in FG consisted of Cyperaceae, Marantaceae, and *Heliconia* herbs and panicoid and oryzoid grasses, with an overall high abundance of grass phytoliths (44).

The pollen concentration of the PN15 sample is much higher than in Unit A (around 20,600 grains cm^{-3}), with a high relative abundance of Poaceae (49%) and Spermacoceae (36%) pollen,

indicative of open and disturbed vegetation (Fig. 3 L–Q) prior to 45 ka cal B.P. in the ELA4 area (Fig. 4B). Many Poaceae pollen grains are relatively large (50 to 64 μm), furthering the presence of Panicoideae and Bambusoideae grass phytoliths. Mangrove (2.4%) and tree (3.5%) pollen grains are rare (SI Appendix, Table S17). Conversely, the large amount of charred plant fragments (“microcharcoals”) in the pollen slides is notable. The high number of macro-charcoals and high percentage of burned phytoliths indicate recurring fires at the site during the concerned time interval, i.e., prior to 47 ka cal B.P. (age of the base of the overlying Unit C; see below), and further consistent with a glacial stadial (MIS 4: 72 to 58 ka; Fig. 4D).

Unit C (47 to 1 ka), Dry/swamp Forest and Savanna to Coastal Savanna and Chenier Plain. Only macroscopic charcoals were hand-picked at KOU-AR6-04, in several levels from Unit C, spanning the 47 to 1 ka time interval (MIS 3c–1). More than 60 fragments, some of them from tree stumps, were retrieved in a brown conglomerate (“Mid”), ^{14}C -dated at $47,053 \pm 572$ cal B.P. They attest to the most speciose tree community uncovered here through charcoals, with at least 15 distinct tree taxa (SI Appendix, Table S15). *Mouriri* sp. is the most abundant tree, followed by *Chaunochiton kappleri* and a close relative, two close allies of *Stryphnodendron*, two unidentified Chrysobalanaceae, Lecythidaceae, cf. Anacardiaceae/Burseraceae and ipê. Just above, floodplain deposits and a silty litter dated at $43,091 \pm 284$ cal B.P. yielded charcoals of unidentified affinities and bootlace tree, respectively. The top levels, dated from the last millennia (^{14}C ages of $1,938 \pm 120$ and 804 ± 55 cal B.P.), yielded charcoals of unidentified Anacardiaceae/Burseraceae, hog plum, cf. Chrysobalanaceae, *Mabea* sp. in the older layer and bootlace tree, Rubiaceae anatomically close to batahua, as well as unidentified Chrysobalanaceae and Leguminosae in the younger one. Pollen and phytoliths were neither sampled nor investigated in Unit C, except for the last millennia (35).

Local Landscape Evolution Since the LIG (Fig. 4 A–C). The marine unit represented in Unit A (Fig. 4A) documents a very short high sea-level interval spanning the LIG [most likely MIS 5e, 128 to 116 ka (9)]. *Rhizophora* trees and *Acrostichum* ferns nowadays only thrive in stable and mature mangroves (46). Their dominance in the pollen assemblages (including pollen clumps) and as charcoals at the base of Unit A suggests that a mangrove ecosystem occurred in the close surroundings (SI Appendix, Tables S15 and S16). Pollen recovery further attests to the existence of montane (e.g., *Alnus*, probably Andean-sourced) and lowland swamp-forest trees, herb, and vines. This is supported by the recognition of dry-forest and back-mangrove tree charcoals (Chrysobalanaceae and Myrtaceae; Fig. 4A). Aquatic communities confirm the proximity of a mangrove belt (e.g., mangrove oysters, decapods, and foraminifers), with shallow-water marine habitats occurring near the sampling points (around 5-m depth), as supported by the co-occurrence of many mollusks. A certain habitat disparity can be inferred from coeval samples, with softer substrates at KOU-AR6-01 than at other loci (abundant spatangoid urchins) or more wave- or tide-related energy in KOU-AR6-06 and -05 Top than anywhere else—high proportion of broken specimens and solitary corallites—thereby pointing to disturbed settings. This landscape strongly recalls the environments of Marajó Island in the Amazon delta and marginal islands with strong marine and tidal influence, as furthered by the co-occurrence of various bony fish taxa with ana-, amphi- or catadromous life cycles (SI Appendix, Table S14). Contrastingly, this type of highly speciose shallow-water environments is not recorded in FG today (20, 47). The local and regional topographies at our sites are consistent with

the ocean being open at the northeast, with terra-firma forests to the southwest (Figs. 1 and 4A). Detrital elements sourced from the continent, through small freshwater streams, as shown by the presence of a synbranchid swamp eel, as well as erythrinid and non-ariid catfish specimens in several loci (Dataset S2).

By ca. 110 ka, the sea had already retreated, as the marine fossils are reworked or oxidized in most trenches, in good agreement with the global eustatic history (Fig. 4D). The microfossil content of the level topping the marine sequence, with only siliceous/phosphatic fossil remains of marine origin (*Discradisca* brachiopods and fish teeth), points to a differential preservation and a post-burial dissolution of calcareous specimens (including foraminifers) in marine deposits posteriorly pedogenetized. Phytoliths sampled in the very top of Unit A point to continental affinities, with the first conspicuous occurrence of grass phytoliths recorded in the PN14 sample. The iron crust topping this unit at various loci further suggests intense surface weathering during a short time (Fig. 1). Afterward, the Kourou sites registered a strong continental signature through pollen, phytoliths, and charcoal, indicating extensive plain savanna to dry forest fringed conditions (Units B and C; Fig. 4 B and C). The occurrence of natural (i.e., pre-human) fires is revealed by burnt phytoliths (ca. 28%) and microcharcoals at KOU-AR6-06-PN15, and by macro-charcoals before 47 ka cal B.P. This suggests that a dry interval may have occurred regionally, perhaps coinciding with a glacial interval (possibly MIS 4).

Charcoals suggest that tree diversity culminated ca. 47 ka cal B.P., in the transition zone between a savanna and a coastal/swamp/riparian forest, or a mosaic of habitats including dryland forest. The presence of bootlace tree might attest to the presence of a swamp forest in the surroundings by 43 ka cal B.P., >100 km away from the coastline (Fig. 4B).

After a gap in the charcoal record, the 2-ka old level at KOU-AR6-04 yields clues of wet-plain and riparian habitats, with *Mabea* and hog plums. The latter tree, with edible fruits (mombin), might also be related to human occupation, documented in the area at that time (36). The youngest charcoal sample (ca. 800 cal B.P.) points to a swamp or riparian forest. The absence of phytolith and pollen record in Unit C impedes characterizing further the last pre-Columbian seasonally flooded local savannas (35).

LIG Marine Communities from KOU-AR6: Taxonomic Diversity and Ecological Affinities.

The estimated sea surface temperature for the Guiana Basin during the LIG was higher (28.9 °C) than today [28.1 °C (45)] (Fig. 4D). Warm periods (e.g., today and LIG) are characterized by an equatorial depletion of marine diversity, with diverse-most areas shifting toward higher latitudes, due to equatorial temperatures being higher than the physiological tolerance of certain species (11, 15, 16): brachyurans, bivalves and gastropods are particularly thermo-sensitive, and today their species diversity decreases in waters exceeding 20 °C (17). To assess the diversity of KOU-AR6 metazoan paleocommunities by the warm LIG, we used a comprehensive survey performed in the 1950s for recent marine organisms of FG as a reference (47). We compared species and genus diversity against depth range and type of substrate (mud, muddy sands, dead shells, and sands), for corals, mollusks (gastropods, bivalves, and scaphopods), brachyuran decapods, echinoderms (sea stars and urchins), and bony fish. We chose this 1950s survey as i) it is unparalleled as a sampling effort and ii) it was undertaken before the last decades’ massive erosion of marine biodiversity of anthropogenic origin (48). As a result, only sea stars denote a lower cumulative diversity in the LIG than in recent samples of compatible substrates and wider bathymetric range (SI Appendix, Table S18). Despite a comparatively limited sampling effort, further restricted by a ca. 5-m-deep depositional setting (unfavorable to the development of

species-rich assemblages), corals, brachyurans, urchins, and bony fish have a similar alpha-diversity in the Kourou LIG samples and in recent samples, while KOU-AR6 mollusk alpha-diversity widely exceeds FG's recent one (twice to four times higher; *SI Appendix, Table S18*). This disparity in molluscan species richness may in part be due to the time-averaging of skeletonized components in death assemblages, accumulating over hundreds to thousands of years along the FG shoreline prior to anthropogenic impacts. Changing environmental factors allowed different species to inhabit these estuarine and coastal areas as time passed, with those death assemblages accumulating an ever-increasing species richness (49, 50).

Indeed, temperature does not explain the entire history of tropical marine diversity (14) and causes may be multiple for this coastal diversity drop between the LIG and the 1950s in FG, notably due to the large-scale marine retreat that occurred meanwhile and exhumed most of the Guianese continental shelf during the LIG (Fig. 4). At a shorter timescale, the shallow marine areas of FG have also experienced deep changes in terms of coastal environment and substrates over the last centuries, with mangroves and mudbanks—characterized by low taxonomic richness and high substrate homogeneity—spreading northwestward all over clear waters. This massive siltation is mainly due to the AP, a huge coastal flux of warm, hyposaline, nutrient-rich, and turbid surface waters of Andean-Amazonian origin (25). This flow plays today a prominent role as a barrier between Brazil and the Caribbean for a wide array of marine animals, including reef fish and gastropods (26, 27). Indeed, its influence on biotic communities over the last interglacials is unknown (25–27). We used the recent geographic distribution of mollusk species recognized at KOU-AR6 as a proxy for testing the ecological affinities of this coastal Guianese fossil assemblage (*Datasets S2 and S3* and Fig. 4). As a result, the closest relationships are retrieved between KOU-AR6 and recent mollusk communities from the Guianas, with 53 species in common. While these Guianese communities tightly group with a Southwestern and South Caribbean cluster, with Eastern Brazil as an offshoot (*SI Appendix, Fig. S14*), they have restricted affinities with the Amazon and Northeastern Brazil living communities. This somewhat contrasts with today's spatial pattern, where Guianese coastal communities are both impoverished and diverging taxonomically from the Caribbean ones, under the major influence of the AP (27). This result suggests that the spatial distribution of Western Atlantic tropical mollusks was not fully shaped by a barrier prefiguring the AP around LIG times, either related to salinity, turbidity, nutrient-balance, or temperature discrepancies. The virtual lack of fossil record documenting this penultimate warm period near the equator (Fig. 1A) impedes getting a broader picture on this very issue, but it clearly highlights where sampling efforts should increase in the future.

Inputs for Conservation Biology and Perspectives for the Near Future. About 30 recent species, among foraminifers, cnidarians, sharks, bryozoans, brachiopods, and mollusks (14 species), have their first and/or earliest fossil record in LIG deposits at KOU-AR6 (*Dataset S2*), which significantly adds to their knowledge and may help for conservation policies (13). Most vertebrate taxa recognized in KOU-AR6 still inhabit FG seawater today, as endemic species of the Central-South American Atlantic coasts (e.g., *Isogomphodon oxyrinchus*, *Carcharhinus porosus*, and *Sphyrna media*; *SI Appendix, Tables S13 and S14*). Due to overfishing, the sawfish, the smalltail, daggernose, and scoophead sharks are critically endangered while the *Albula vulpes* bonefish is nearly threatened and the *Cynoscion acoupa* weakfish is vulnerable (*Dataset S2*). The presence of these species 125 ka ago in the same area and their current small range (*Dataset S2*) suggest low mobility on 10^5 to 10^6 -year timescales, as predicted by spatial distribution models (13, 51). It would also be indicative of

higher vulnerability to overfishing than to warming for these taxa (15–17). As such, this study on past communities may open unique perspectives regarding in-depth taxonomic studies, community ecology analyses, and extinction risks of the considered assemblages. Hopefully, future records would follow and help bridging stratigraphic and biogeographic gaps on a regional scale (14).

Environmental conditions during the climax of MIS 5e strikingly echo the most pessimistic scenarios for global warming and sea-level rise in 2100 AD, notably in Central and South America (45, 52). This analogy has a particular resonance, as the Guianese coastal areas located at less than 10 m above modern sea level are critically concerned by the current sea-level and temperature rises and subsequent cascading risks, such as vector-borne disease epidemics, and drastic changes in Amazon biome dynamics (52–54). Indeed, low-elevation coastal zones hosting around 20, 55 and 80% of FG, Guyana, and Suriname inhabitants, respectively, are at risk of being entirely flooded before 2100 AD (52, 55, 56), as are irremovable infrastructures of the area (e.g., airports and Europe's Spaceport). As the future may be learned from the past in terms of marine biodiversity and coastal ecosystem dynamics and fate (16, 48, 57), we hope that the present work would help raise collective awareness of the major environmental upheavals that the region may experience in the next century, especially for decision-makers, whether local or transnational.

Materials and Methods

The material was collected through handpicking (charcoals) and screen-washing of more than one metric ton of sediments [with 2 mm, 1 mm, and 0.7 mm meshes for most fossil groups and smaller meshes for microvertebrates (0.4 mm) and foraminifers (150 and 63 μ m)]. The fossil specimens belong to the collections of the Université de Guyane in Cayenne. When large numbers of specimens were available for a given species, other specimens have been further stored in the collections of the Université de Montpellier.

Age constraints were provided through U-Th datings on corals (Unit A), OSL dating on quartz grains (Units A and B) and 14 C datings (Unit C).

Taxonomic identifications were undertaken by recognized specialists of each group of interest, aiming at retaining the most accurate and conservative assignment level. These assignments range from species to family level, highly depending on completeness of the concerned KOU-AR6 records and/or on current knowledge discrepancies about recent taxa themselves (*SI Appendix, Tables S7–S17*).

For comparing the diversity of KOU-AR6 past communities (five marine samples over a 0.5-km² surface at a ca. 5-m depth; this work), we used a comprehensive survey (47) performed in 1954 to 1957 on recent marine organisms on the Guianese Continental Plate (400 samples over ca. 40,000 km², including 110 samples for a 0 to 29-m depth range and 272 for a 20 to 49-m depth range) on compatible substrates and a wider bathymetric range (mud, 0 to 30-m depth; muddy sands, dead shells, and sands, 20 to 49-m depth).

To define the ecological affinities of KOU-AR6 LIG mollusks at the Western Atlantic scale, a taxon/area matrix, widely inspired from that of a recent biogeographic analysis (27), was built for the 74 species having a well-defined distribution area today (*Datasets S2 and S3*). For that, we used the mapper tool of the Ocean Biodiversity Information System repository (<https://mapper.obis.org>), completed by an atlas of FG's mollusks (58). We then ran UPGMA and parsimony analyses with PAUP* 4.0a.169 (59).

Data, Materials, and Software Availability. All study data are included in the article and/or [supporting information](#).

ACKNOWLEDGMENTS. We are grateful to Nils Stenseth (invited editor), but also to Moriaki Yasuhara and an anonymous reviewer for their constructive and stimulating remarks on previous versions of the manuscript. We are deeply indebted to François Catzeffis for paving the way to this French Guianese fossil record, to Martijn van den Bel and everybody at INRAP in Cayenne-Matoury for granting access to their facilities in 2018, to Michel Brossard, Michel Macarit, and Lionel

Hautier for their participation to preliminary field and screen-washing operations, to Carlos Jaramillo for preparing early samples and for fruitful discussion, and to Henry Hooghiemstra for providing relevant suggestions on our manuscript. We are particularly thankful to the Centre National d'Etudes Spatiales (Sandrine Richard and Henri Brunet-Lavigne), the Centre Spatial Guyanais, Eiffage (Henri Beny), and Sodexo (Patrick Raverat). This work was funded by the French Agence Nationale de la Recherche (ANR) in the framework of both the LabEx CEBA (ANR-10-LABX-25-01), through the projects Source, NeotroPhyl, Timespan and Emergence, and the GAARAnti project (ANR-17-CE31-0009). O.A. acknowledges funding from the Brazilian Council of Science and Technological Development (CNPq 304693/2021-9). N.H.W. acknowledges funding from the European Research Council (ERC 2019 StG 853394). R.J.-B acknowledges funding from the Australian Research Council (ARC DP220100195 and LE200100022). P.G.V. acknowledges funding from the French ANR-PIA program (ANR-18-MPGA-0006). This is ISEM-Sud article no. 2024-051.

Author affiliations: ^aEquipe de Paléontologie, Institut des Sciences de l'Évolution de Montpellier, Univ Montpellier, CNRS, Institut de Recherche pour le Développement, Montpellier 34095, France; ^bPaleoecology and Global Changes Laboratory, Marine Biology Department, Fluminense Federal University, Niterói 24210-201, Rio de Janeiro, Brazil; ^cDepartment of Paleoanthropology, Senckenberg Research Institute, Frankfurt am Main 60325, Germany; ^dDepartment of Invertebrate Zoology, Smithsonian Institution, National Museum of Natural History, Washington D.C. 20013-7012; ^eDepartamento de Ciencias del Mar y Limnología, Universidad Nacional Autónoma de México, Coyoacán, Ciudad de México 04510, México; ^fEquipe Dynamique de la Lithosphère, Géosciences Montpellier, Univ Montpellier, CNRS, Montpellier 34095, France; ^gMass Spectrometry

- H. P. Comes, J. W. Kadereit, The effect of Quaternary climatic changes on plant distribution and evolution. *Trends Plant Sci.* **3**, 432–438 (1998).
- M. Dynesius, R. Jansson, Evolutionary consequences of changes in species' geographical distributions driven by Milankovitch climate oscillations. *Proc. Natl. Acad. Sci. U.S.A.* **97**, 9115–9120 (2000).
- W. B. Ludt, L. A. Rocha, Shifting seas: The impacts of Pleistocene sea-level fluctuations on the evolution of tropical marine taxa. *J. Biogeogr.* **42**, 25–38 (2015).
- L. B. Railsback *et al.*, An optimized scheme of lettered marine isotope substages for the last 1.0 million years, and the climatostratigraphic nature of isotope stages and substages. *Quat. Sci. Rev.* **111**, 94–106 (2015).
- R. M. Spratt, L. E. Lisiecki, A Late Pleistocene sea level stack. *Clim. Past* **12**, 1079–1092 (2016).
- P. Gresse *et al.*, Beachrocks of the last low sea level, substrate of the Great Amazon Reef system along the outer Guiana shelf. *Geo-Marine Lett.* **43**, 10 (2023).
- A. Dutton, K. Lambeck, Ice volume and sea level during the last interglacial. *Science* **337**, 216–219 (2012).
- A. Rovere *et al.*, The analysis of Last Interglacial (MIS 5e) relative sea-level indicators: Reconstructing sea-level in a warmer world. *Earth-Sci. Rev.* **159**, 404–427 (2016).
- P. L. Gibbard, M. J. Head, *The Quaternary period*. In *Geologic Time Scale 2020*, F. M. Gradstein, J. G. Ogg, M. D. Schmitz, G. M. Ogg, Eds. (Elsevier, 2020), pp. 1217–1255.
- K. Rubio-Sandoval *et al.*, A review of last interglacial sea-level proxies in the western Atlantic and southwestern Caribbean, from Brazil to Honduras. *Earth Syst. Sci. Data* **13**, 4819–4845 (2021).
- W. Kiessling *et al.*, Equatorial decline of reef corals during the last Pleistocene interglacial. *Proc. Natl. Acad. Sci. U.S.A.* **109**, 21378–21383 (2012).
- A. Rovere *et al.*, The World atlas of last interglacial shorelines (version 1.0). *Earth Syst. Sci. Data* **15**, 1–23 (2023).
- S. Finnegan *et al.*, Using the fossil record to understand extinction risk and inform marine conservation in a changing world. *Ann. Rev. Marine Sci.* **16**, 1–27 (2023).
- M. Yasuhara *et al.*, Hotspots of Cenozoic tropical marine biodiversity. *Oceanogr. Mar. Biol.* **60**, 243–300 (2022).
- O. Rama-Corredor *et al.*, Parallelisms between sea surface temperature changes in the western tropical Atlantic (Guiana Basin) and high latitude climate signals over the last 140 000 years. *Clim. Past* **11**, 1297–1311 (2015).
- M. Yasuhara *et al.*, Past and future decline of tropical pelagic biodiversity. *Proc. Natl. Acad. Sci. U.S.A.* **117**, 12891–12896 (2020).
- M. Yasuhara, C. A. Deutsch, Paleoecology provides glimpses of future ocean: Fossil records from tropical oceans predict biodiversity loss in a warmer world. *Science* **375**, 25–26 (2022).
- The Paleoecology Database, Download Records. http://paleobiodb.org/data1.2/occs/list.csv?datainfo&rowcount&base_name=Mollusca&interval=Middle%20Pleistocene.Late%20Pleistocene&cc=AFR,EUR,NOA,SOA&latmin=-60&latmax=60. Accessed 29 November 2023.
- J. Boggan *et al.*, *Checklist of the Plants of the Guianas* (Museum of Natural History, Smithsonian Institution, Smithsonian's Biological Diversity of the Guianas Program series 30, ed. 2, 1997).
- L.-F. Artigas *et al.*, Marine biodiversity in French Guiana: Estuarine, coastal, and shelf ecosystems under the influence of Amazonian waters. *Gayana* **67**, 302–326 (2003).
- A. Sánchez Meseguer *et al.*, Diversification dynamics in the Neotropics through time, clades, and biogeographic regions. *Elife* **11**, e74503 (2022).
- A. K. Gibbs, C. N. Barron, F. Tabart, *The Geology of the Guiana Shield* (Oxford University Press, New York, 1993), vol. **246**.
- P.-O. Antoine *et al.*, Un inventaire fossile de la Guyane: Historique et nouvelles perspectives. *Géologues* **206**, 28–30 (2020).
- J. C. Lindeman, The vegetation of the Coastal Region of Suriname. Results of the scientific expedition to Suriname 1948–49 botanical series No. 1. *Meded. Bot. Mus. Herb. Rijks Univ. Utrecht* **113**, 1–135 (1952).

Laboratory, Center for Physical Sciences and Technology, Vilnius 10257, Lithuania; ^hGeomar, Helmholtz Centre for Ocean Research Kiel, Kiel 24148, Germany; ⁱInstitute of Geological Sciences, Oeschger Centre for Climate Change Research, University of Bern, Bern 3012, Switzerland; ^jArchéozoologie et Archéobotanique—Sociétés, Pratiques et Environnements, CNRS, Muséum National d'Histoire Naturelle, Paris 75005, France; ^kInvertebrate Paleontology Department, Natural History Museum of Los Angeles County, Los Angeles, CA 90007; ^lEcosystem & Landscape Dynamics Department, Institute for Biodiversity and Ecosystem Dynamics, Universiteit van Amsterdam, Amsterdam 1098 XH, The Netherlands; ^mGeoarchaeology and Archaeometry Research Group, Southern Cross GeoScience, Southern Cross University, East Lismore, NSW 2480, Australia; ⁿCentre for Anthropological Research, University of Johannesburg, Johannesburg 2092, South Africa; ^oArbeitsgruppe Mikropaläontologie, Institut für Geowissenschaften, Paläontologie, Universität Bonn, Bonn 53115, Germany; ^pDepartment of Zoology, Museum of Zoology, University of Cambridge, Cambridge CB2 3EJ, United Kingdom; ^qDepartment of Historical Geology-Paleontology, National and Kapodistrian University of Athens, Panepistimiopolis, Zografou, Athens 15784, Greece; ^rLaboratoire de Géologie de Lyon - Terre, Planètes, Environnement, Université Claude Bernard Lyon 1, Ecole Normale Supérieure de Lyon, CNRS, Villeurbanne F-69622, France; ^sSection Systems Ecology, Amsterdam Institute for Life and Environment, Vrije Universiteit, Amsterdam 1081 BT, The Netherlands; ^tEquipe Tectonique, Reliefs et Bassins, Institut des Sciences de la Terre, Université Grenoble Alpes, Université Savoie Mont Blanc, CNRS, Université Gustave Eiffel, Grenoble 38058, France; ^uDépartement Formation et Recherche Sciences et Technologie, Université de Guyane, Cayenne 97300, Guyane; ^vOnikha, Kourou 97310, Guyane; and ^wOffice de l'Eau de Guyane, Cayenne 97300, Guyane

Author contributions: P.-O.A. and A. Heuret designed research; P.-O.A., L.N.W., S.A., O.A., S.C.B., S. Cairns, C.A.C.-V., J.-J.C., N.O.G., S.G., A. Hendy, C.H., R.J.-B., M.R.L., J.L., L.M., P.M., K.N., F.Q., M.S., P.G.V., N.H.W., A.C., S. Clavier, P.B., M.G., M.R., and A. Heuret performed research; P.-O.A., L.N.W., S.A., O.A., S.C.B., J.-J.C., Ž.E., J.F., N.O.G., S.G., A. Hendy, C.H., R.J.-B., M.R.L., J.L., P.M., K.N., F.Q., J.S., M.S., P.G.V., and N.H.W. analyzed data; P.-O.A., M.G., and M.R. performed fieldwork; L.N.W., O.A., S.C.B., S. Cairns, C.A.C.-V., Ž.E., J.F., N.O.G., S.G., A. Hendy, C.H., M.R.L., J.L., P.M., K.N., F.Q., J.S., and N.H.W. contributed to writing; L.N.M., S.A., J.-J.C., M.S., A.C., S. Clavier, P.B., and A. Heuret performed fieldwork, contributed to writing; and P.-O.A. wrote the paper.

- M. Pujos, J.-M. Froidefond, Water masses and suspended matter circulation on the French Guiana continental shelf. *Contin. Shelf Res.* **15**, 1157–1171 (1995).
- S. R. Floeter *et al.*, Atlantic reef fish biogeography and evolution. *J. Biogeogr.* **35**, 22–47 (2008).
- E. Giachini Tosetto, A. Bertrand, S. Neumann-Leitão, M. Nogueira Júnior, The Amazon River plume, a barrier to animal dispersal in the Western Tropical Atlantic. *Sci. Rep.* **12**, 537 (2022).
- M. Mestre, S. Delpech, *Plateau des Mines* (Excavation report, Saint-Laurent du Maroni, INRAP, Cayenne, 2008).
- G. Odonne *et al.*, Long-term influence of early human occupations on current forests of the Guiana Shield. *Ecology* **100**, e02806 (2019).
- M. G. Plew, L. Daggars, *The Archaeology of Guyana* (University of Guyana Press, ed. 2, 2022).
- E. Palvadeau, *Géodynamique quaternaire de la Guyane Française* (BRGM, Université de Bretagne Occidentale, 1999), p. 255.
- G. Brunier *et al.*, Evolution of the French Guiana coast from Late Pleistocene to Holocene based on chenier and beach sand dating. *Region. Envir. Change* **22**, 122 (2022).
- P. U. Clark *et al.*, The last glacial maximum. *Science* **325**, 710.e714 (2009).
- C. J. Van Meerbeek, H. Renssen, D. M. Roche, How did marine isotope stage 3 and last glacial maximum climates differ?—Perspectives from equilibrium simulations. *Clim. Past* **5**, 33–51 (2009).
- J. Iriarte *et al.*, Fire-free land use in pre-1492 Amazonian savannas. *Proc. Natl. Acad. Sci. U.S.A.* **109**, 6473–6478 (2012).
- M. M. van den Bel, Nouveaux apports sur l'archéologie du littoral de Guyane: De la préhistoire à la conquête. *J. Soc. Am.* **104**, 105–152 (2018).
- N. Sariaslan, M. R. Langer, Atypical, high-diversity assemblages of foraminifera in a mangrove estuary in northern Brazil. *Biogeosci.* **18**, 1–18 (2021).
- A. C. S. Almeida, F. B. C. Souza, L. M. Vieira, Malacostegine bryozoans (Bryozoa: Cheilostomata) from Bahia State, northeast Brazil: Taxonomy and non-indigenous species. *Marine Biodiv.* **48**, 1463–1488 (2017).
- L. M. Vieira, A. E. Migotto, J. E. Winston, Synopsis and annotated checklist of Recent marine Bryozoa from Brazil. *Zootaxa* **1810**, 1–39 (2008).
- D. J. Hughes, J. B. C. Jackson, Do constant environments promote complexity of form?: The distribution of bryozoan polymorphism as a test of hypotheses. *Evolution* **44**, 889–905 (1990).
- T. Van der Hammen, A palynological study on the Quaternary of British Guiana. *Leidse Geol. Meded.* **29**, 125–180 (1963).
- R. M. Piperno, *Phytoliths: A Comprehensive Guide for Archaeologists and Paleoecologists* (Rowman Altamira, 2006).
- C. Crifó, C. A. Strömberg, Small-scale spatial resolution of the soil phytolith record in a rainforest and a dry forest in Costa Rica: Applications to the deep-time fossil phytolith record. *Palaeogeogr. Palaeoclimatol. Palaeoecol.* **537**, 109107 (2020).
- J. Iriarte *et al.*, Late Holocene Neotropical agricultural landscapes: Phytolith and stable carbon isotope analysis of raised fields from French Guianan coastal savannas. *J. Archaeol. Sci.* **37**, 2984–2994 (2010).
- J. B. C. Jackson *et al.*, Historical overfishing and the recent collapse of coastal ecosystems. *Science* **293**, 629–637 (2001).
- S. Guitet, R. Pélissier, O. Brunaux, G. Jaouen, D. Sabatier, Geomorphological landscape features explain floristic patterns in French Guiana rainforest. *Biodiv. Conserv.* **24**, 1215–1237 (2015).
- J. Durand, Notes sur le plateau continental guyanais: Les éléments principaux de la faune et leurs relations avec le fond. *Cah. ORSTOM* **3**, 1–99 (1959).
- C. Chaudhary *et al.*, Global warming is causing a more pronounced dip in marine species richness around the equator. *Proc. Natl. Acad. Sci. U.S.A.* **118**, 1–6 (2021).
- G. M. Staff, E. N. Powell, The paleoecological significance of diversity: The effect of time averaging and differential preservation on macroinvertebrate species richness in death assemblages. *Palaeogeogr. Palaeoclimatol. Palaeoecol.* **63**, 73–89 (2008).

50. A. Tomašových, S. M. Kidwell, Fidelity of variation in species composition and diversity partitioning by death assemblages: Time-averaging transfers diversity from beta to alpha levels. *Paleobiol.* **35**, 94–118 (2009).
51. C. J. Reddin *et al.*, Victims of ancient hyperthermal events herald the fates of marine clades and traits under global warming. *Glob. Change Biol.* **27**, 868–878 (2021).
52. I. Hagen *et al.*, Climate change-related risks and adaptation potential in Central and South America during the 21st century. *Environ. Res. Lett.* **17**, 033002 (2022).
53. J. Barlow *et al.*, The future of hyperdiverse tropical ecosystems. *Nature* **559**, 517–526 (2018).
54. B. Neumann, A. T. Vafeidis, J. Zimmermann, R. J. Nicholls, Future coastal population growth and exposure to sea-level rise and coastal flooding—a global assessment. *PLoS One* **10**, e0118571 (2015).
55. A. Heuret, S. Bodin, L. Marivaux, P.-O. Antoine, Des étoiles aux fossiles. Quand Ariane 6 dévoile la Guyane pléistocène. *Une saison en Guyane* **7**, 4–9 (2021).
56. G. McGranahan, D. Balk, B. Anderson, The rising tide: Assessing the risks of climate change and human settlements in low elevation coastal zones. *Environ. Urban.* **19**, 17–37 (2007).
57. H. K. Lotze, L. McClenachan, "Marine historical ecology: Informing the future by learning from the past" in *Marine Community Ecology and Conservation*, M. D. Bertness *et al.*, Eds. (Sinauer Associates Inc, Sunderland, 2014), pp. 165–200.
58. D. Massemin, D. Lamy, J.-P. Pointier, O. Gargominy, *Coquillages et escargots de Guyane* (Publications Scientifiques du Muséum, MNHN, Paris, 2009).
59. D. Swofford, PAUP*. Phylogenetic Analysis Using Parsimony (*and Other Methods), version 4.0a.169 (Sinauer Associates, Sunderland, 2002). <https://phylosolutions.com/paup-test/>. Accessed 18 December 2023.